Supplementary Information

Unveiling the Membrane-Binding Properties of N-terminal and C-terminal Regions of G Protein-Coupled Receptor Kinase 5 by Combined Optical Spectroscopies

Bei Ding, Alisa Glukhova, Katarzyna Sobczyk-Kojiro, Henry I. Mosberg, John J. G. Tesmer, Zhan Chen

Supplemental Figures

Figure S1. Experimental geometry of SFG signal detection

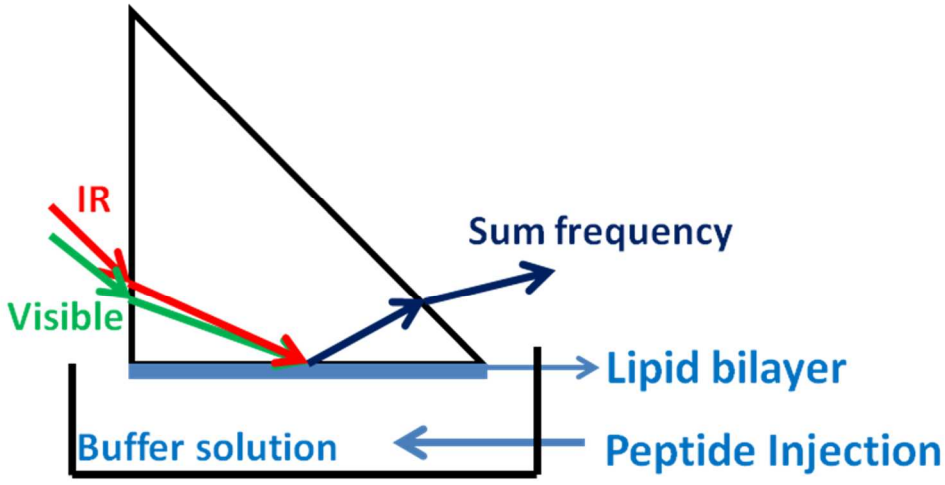

Figure S2. Influence of PIP_2 on membrane binding properties of GRK5 peptides. (a) SFG signals in the C-H and O-H stretching frequency region detected from the interface between the POPC:PIP_2 (9:1) lipid bilayer and buffer alone (black), upon addition of $GRK5_{2–31}$ in 10 mM phosphate buffer pH 7.4 (red), after washing (blue), and in 60% buffer/40% TFE (dark cyan). (b) SFG signals in the amide I frequency region from $GRK5_{2–31}$ associated with a POPC:PIP_2 (9:1) bilayer in contact with peptide solution in 10 mM 60% phosphate buffer pH 7.4/40% TFE. (c) SFG signals in the amide I frequency region from $GRK5_{2–31}$ associated with a POPC:PIP_2 (9:1) bilayer in contact with 60% PBS buffer/40% TFE. (d) SFG signals in the C-H and O-H stretching frequency region from the interface between the POPC:PIP_2 (9:1) lipid bilayer and buffer alone (black), in the presence of $GRK5_{2–24}$ (red), and 10 mM phosphate buffer after washing (blue) (e) SFG amide I spectra for $GRK5_{546–565}$ associated with a POPC:PIP_2 (9:1) bilayer in 10 mM phosphate buffer pH 7.4.

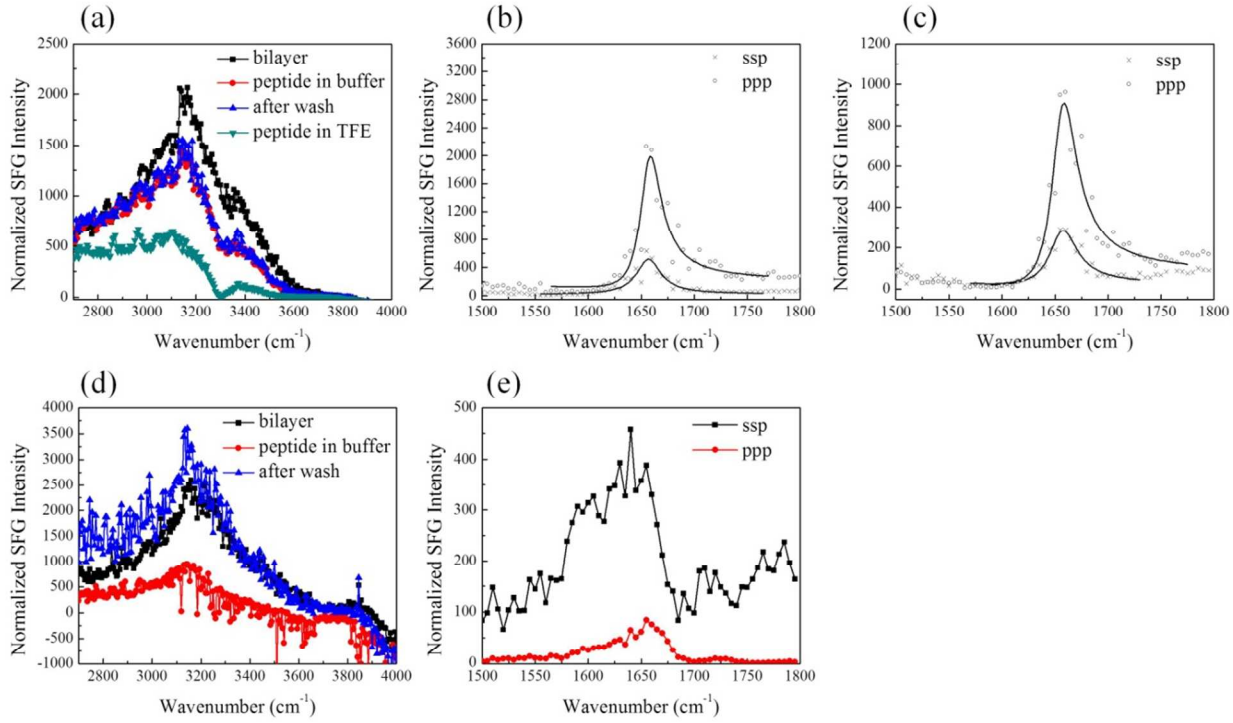

Figure S3. Time dependent SFG signals detected before and after the addition of peptide stock solution to the subphase at about 200 s. (a) $GRK5_{2–31}$ in phosphate buffer, (b) $GRK5_{2–31}$ in PBS buffer, (c) $GRK5_{2–24}$ in phosphate buffer, (d) $GRK5_{25–31}$ in phosphate buffer (e) $GRK5_{546–565}$ in phosphate buffer

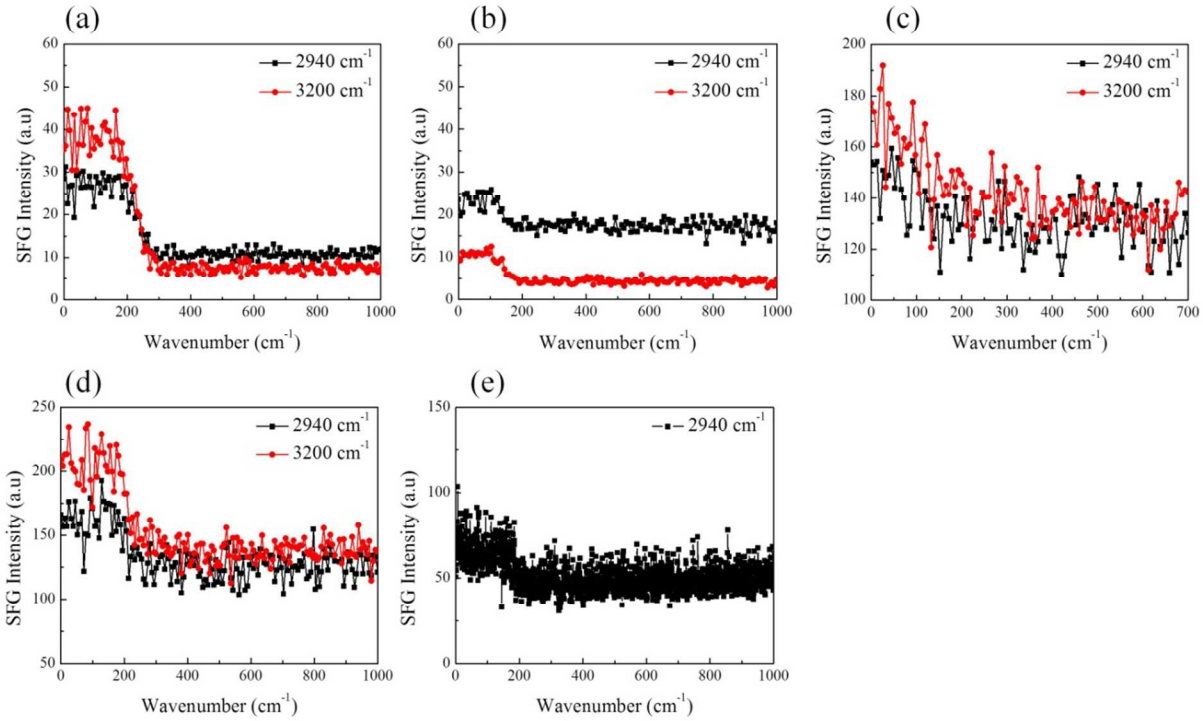

Figure S4. ATR-FTIR spectra detected from $GRK5_{2–31}$ associated with a POPC lipid bilayer in contact with 40% TFE/ 60% 10 mM phosphate buffer pH 7.4.

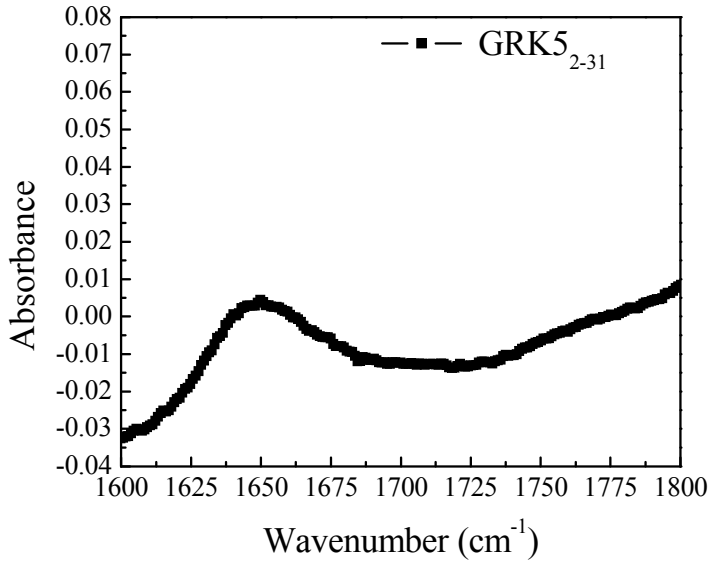

Figure S5: ATR-FTIR signals detected before and after the addition of equimolar CaM·Ca^{2+} to the subphase for $GRK5_{25–31}$. ATR-FTIR spectra represent signals collected from peptides associated with the lipid bilayer before (black), after washing (red), after the addition of CaM·Ca^{2+} to the subphase (blue), and after subsequent washing (dark cyan).

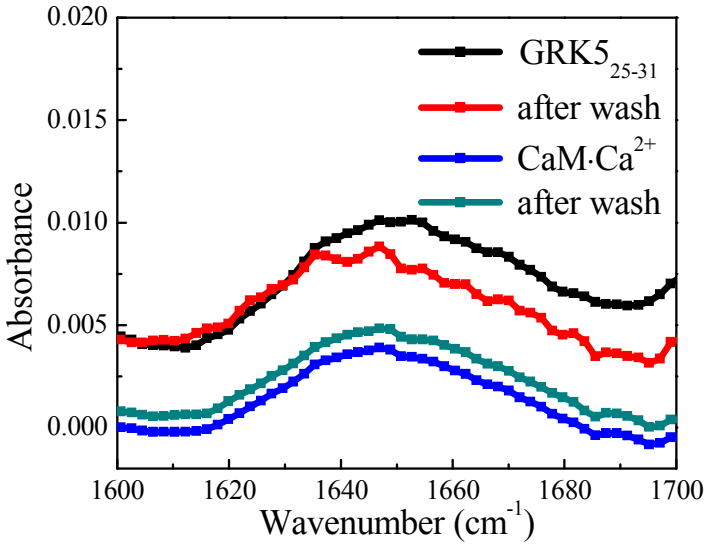

Figure S6: CaM·Ca^{2+} is loosely associated with the POPC lipid bilayer. ATR-FTIR signals detected upon the addition of CaM·Ca^{2+} to the subphase for POPC lipid bilayer before (black), and after (red) washing.

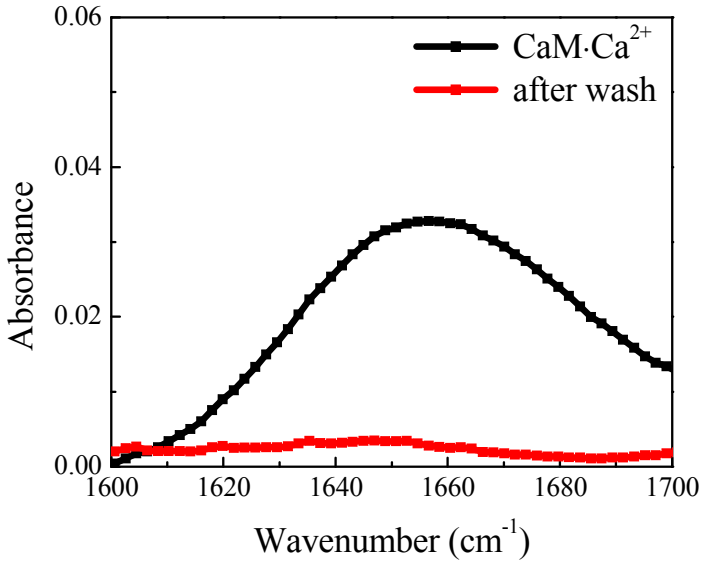

3. SFG Orientation Analysis on Amide I Signals

First, we generated an orientation curve plotting $\chi^{(2)}_{zzz}/\chi^{(2)}_{xxz}$, the ratio of the two susceptibility tensor elements as a function of the tilt angle (which is defined as the angle between the helix axis and the surface normal of the supported lipid bilayer). Second, the intensity of experimental SFG spectra is proportional to the square of the effective second order nonlinear optical susceptibility $\chi^{(2)}_{eff,ppp}$.

$$\chi^{(2)}_{\mathrm{eff}} = \chi^{(2)}_{\mathrm{nr}} + \sum_q \frac{A_q}{\omega_n - \omega_q + i\Gamma_q} \qquad (1)$$

Where $\chi^{(2)}_{\mathrm{nr}}$ denotes the nonresonant background, A_q denotes the signal strength, ω_n and ω_q are frequencies of the tunable IR beam and a specific vibration mode (the peak center), and Γ_q is the damping coefficient. Thus, we can obtain the ratio of the effective second order nonlinear optical susceptibility $\chi^{(2)}_{eff,ppp}/\chi^{(2)}_{eff,ppp}$ value by fitting the ppp and ssp spectra of the amide I region.

Third, the experimental $\chi^{(2)}_{zzz}/\chi^{(2)}_{xxz}$ can be derived from $\chi^{(2)}_{eff,ppp}/\chi^{(2)}_{eff,ppp}$ value after taking consideration of the Fresnel coefficients.

$$\chi^{(2)}_{\mathrm{eff,ssp}} = \mathrm{L_{xxz}}\chi^{(2)}_{\mathrm{xxz}} \qquad (2)$$

$$\chi^{(2)}_{\mathrm{eff,ppp}} = \mathrm{L_{xxz}}\chi^{(2)}_{\mathrm{xxz}} + \mathrm{L_{xzx}}\chi^{(2)}_{\mathrm{xzx}} + \mathrm{L_{zxx}}\chi^{(2)}_{\mathrm{zxx}} + \mathrm{L_{zzz}}\chi^{(2)}_{\mathrm{zzz}} \qquad (3)$$

The experimental $\chi^{(2)}_{zzz}/\chi^{(2)}_{xxz}$ can be used to find the tilt angle with the theoretical orientation curve.